Research article

Multiparametric MR imaging in diagnosis of chronic prostatitis and its differentiation from prostate cancer

Vivek Kumar Sah [a], Liang Wang [a],*, Xiangde Min [a], Zhaoyan Feng [a], Rajiv Rizal [a], Liang Li [a], Ming Deng [a], Jihong Liu [b], Hongjun Li [c]

[a] *Department of Radiology, Tongji Medical College, Huazhong University of Science & Technology, Wuhan 430030, Hubei, PR China*
[b] *Department of Urology, Tongji Medical College, Huazhong University of Science & Technology, Wuhan 430030, Hubei, PR China*
[c] *Department of Radiology, Beijing You An Hospital, Capital Medical University, No 8, Si Tou Tiao, YouAn Men Wai, Feng Tai District, Beijing, 100069, China*

Abstract

Chronic prostatitis is a heterogeneous condition with high prevalence rate. Chronic prostatitis has overlap in clinical presentation with other prostate disorders and is one of the causes of high serum prostate specific antigen (PSA) level. Chronic prostatitis, unlike acute prostatitis, is difficult to diagnose reliably and accurately on the clinical grounds alone. Not only this, it is also challenging to differentiate chronic prostatitis from prostate cancer with imaging modalities like TRUS and conventional MR Imaging, as the findings can mimic those of prostate cancer. Even biopsy doesn't play promising role in the diagnosis of chronic prostatitis as it has limited sensitivity and specificity. As a result of this, chronic prostatitis may be misdiagnosed as a malignant condition and end up in aggressive surgical management resulting in increased morbidity. This warrants the need of reliable diagnostic tool which has ability not only to diagnose it reliably but also to differentiate it from the prostate cancer. Recently, it is suggested that multiparametric MR Imaging of the prostate could improve the diagnostic accuracy of the prostate cancer. This review is based on the critically published literature and aims to provide an overview of multiparamateric MRI techniques in the diagnosis of chronic prostatitis and its differentiation from prostate cancer.

1. Introduction

Prostatitis is one of the common reasons why patients visit physicians and urologists. The prevalence of prostatitis is high, overall rate of 8.2%, which is comparable to rates of ischemic heart disease and diabetes [1]. This necessitates the need for accurate and reliable diagnostic tool. However, there are no specific physical findings or diagnostic laboratory tests to diagnose it. The National Institute of Health (NIH) established an International Prostatitis Collaborative Network (IPCN) and came with 4 categories of prostatitis syndromes viz. I) Acute bacterial prostatitis, II) Chronic bacterial prostatitis, III) Chronic non-bacterial prostatitis/Chronic pelvic pain syndrome (CP/CPPS) which was further categorized into inflammatory (category IIIA) and non-inflammatory (category IIIB), IV) Asymptomatic inflammatory prostatitis [1]. Acute and chronic bacterial prostatitis are best understood among them and are easier to diagnose clinically. Chronic nonbacterial prostatitis is the most common and affect 10−15% of male population [2], however, remains the diagnosis of exclusion. The working diagnostic criteria that is used clinically is the presence of pelvic pain or urinary symptoms for more than three of the previous 6 months with no evidence of

* Corresponding author. Department of Radiology, Tongji Hospital, Tongji Medical College, Huazhong University of Science & Technology, Jie-Fang-Da-Dao 1095, Wuhan 430030, PR China. Tel.: +86 027 83663547 (office), +86 13971625289 (cell).

E-mail addresses: wangliang_2001@yahoo.com, wang6@tjh.tjmu.edu.cn (L. Wang).

Peer review under responsibility of Beijing You'an Hospital affiliated to Capital Medical University.

acute bacterial prostatitis or urinary tract infection in that time [2]. Chronic prostatitis can be a cause of elevated prostate specific antigen (PSA) level. This warrants further investigations as the elevated PSA level should not be attributed to chronic prostatitis without ruling out prostate cancer [3,4]. The current emphasis is on the studies that provide indirect information about the prostate like DRE, Retrograde urethrography, Cystourethroscopy [5]. The reliable and accurate diagnosis has yet been difficult to achieve due to the heterogeneous nature of chronic prostatitis. MRI provides visualization of the interior structure and better delineation of anatomy and prostate pathologic condition. TRUS, CT and conventional MRI are informative but it is difficult to detect and differentiate chronic prostatitis from prostate cancer with these radiological modalities as the findings can mimic those of prostate cancer [6−8]. Multiparametric MRI is better at detecting the prostate cancer with high sensitivity and specificity [9,10]. Multiparametric MRI is also helpful in predicting the presence of prostate cancer in prostate biopsy [11]. It is also helpful in differentiating of prostatitis and prostate cancer [12].

2. Anatomy relevant to chronic prostatitis

MRI is superior to CT, ultrasound or other radiological modalities in delineating the anatomy of prostate and its surroundings. Prostate is a walnut shaped gland, which sits on the urogenital diaphragm in the lower pelvis just inferior to the urinary bladder (Figs. 1 and 2). The anterior wall is separated from the pubic bone by the retropubic fatty space of Retzius. The posterior wall is separated from the rectal ampulla by Denonvillier's fascia. The fluid filled seminal vesicles are situated postero-superior lying between the bladder and the rectum (Fig. 2B). The ejaculatory duct, which is formed after the seminal duct joins the ductus deference, enters the prostate gland posteriorly, runs into it and finally opens on the seminal colliculus (verumontanum) at the utricle of the prostatic urethra. Neurovascular bundles, responsible for erection of the
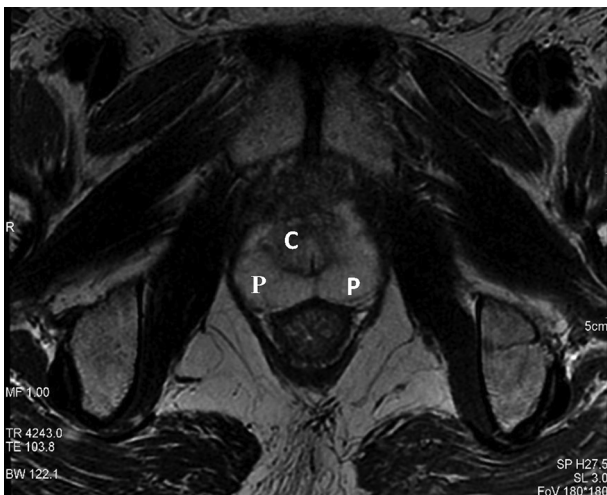

Fig. 1. Axial T2WI showing the zonal anatomy of the prostate. The central gland (C) is shown as heterogeneous signal intensity surrounded by a crescent shaped hyperintense peripheral zone (P) on both sides.

penis, run from superior to inferior in the posterolateral sides of the prostate glands. The prostate gland is divided into base, mid-prostate and apex from superior to inferior (Fig. 2B).

The prostate is divided anatomically into three zones viz. the peripheral, the transition and the central zones (Figs. 1 and 2). Anterior fibromuscular stroma, mainly consisting of muscular and the connective tissue and lacking glandular tissue, is located in the anterior part of the prostate gland. The peripheral zone of the prostate is situated postero-inferiorly and is the most common location for malignancy, around 70−80% of the prostate cancer foci being located in this zone [13,14]. Located interiorly and surrounding the prostatic urethra is the transition zone and postero-superior to it is the central zone. Transition zone is common site for benign prostatic hyperplasia (BPH). The transition and the central zones are together called as internal or central gland, as they are barely distinguishable from one another [15]. Due to the occurrence of benign prostatic hyperplasia with increasing age, the morphology of central gland changes from central zone into transition zone. As nodules in the transition zone advances, the central zone undergoes compression with progressive displacement towards the prostatic base which makes anatomy of the central zone difficult to be defined with confidence by MR Imaging [16] (Fig. 1). Around 20% and 10% of the prostate cancer foci arise from the transition and the central zone, respectively [17]. Chronic prostatitis mainlyoccursin the peripheral zone of prostate and is more demonstrable than acute condition in the context of MRI examination. Chronic prostatitis can be present with symptoms of benign prostatic hyperplasia (BPH). It is also commonly associated with elevated serum prostate specific antigen (PSA). Therefore, it is an important differential in the diagnosis of prostate cancer.

3. MR examinations

Multiparametric prostate MR examination combines both conventional as well as functional MR imaging, and requires at least16 channel1.5 T with endorectal coil or 3.0 T with or without endorectal coil. 3.0 T image acquisition provides better signal-to-noise ratio (SNR) with faster acquisition of high quality image, with or without the use of endorectal coil [18]. However, the longer T1 and shorter T2 relaxation times are the disadvantages with higher field strength of 3.0 T [19].

3.1. T2 weighted MR imaging

T2WI MR Images are used to show anatomy of the prostate and its surrounding structures. The normal appearance of the peripheral zone of the prostate gland is characterized by the homogenous intermediate to high intensity signal (Fig. 3A). The peripheral zone is surrounded by capsule represented as a thin hypointense rim on MR image, which clearly depicts it from the transition and central zone. Lesions of chronic prostatitis, on T2WI MR imaging, usually present with unilateral or bilateral diffuse or flaky areas with little to no mass effect or wedge shaped areas of low signal intensity in the
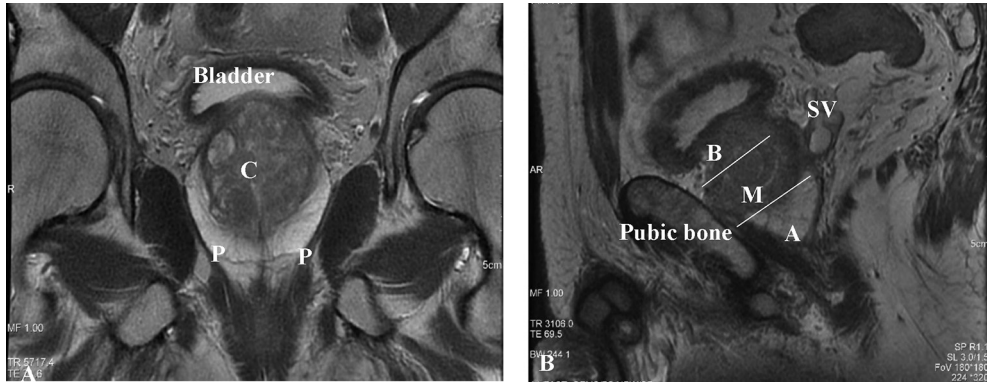
Fig. 2. (A) Coronal T2WI and (B) sagittal T2WI showing cranio-caudal segmentation of the prostate and its surrounding structures. B = Base, M = Mid-prostate, A = Apex, SV = Seminal Vesicles.
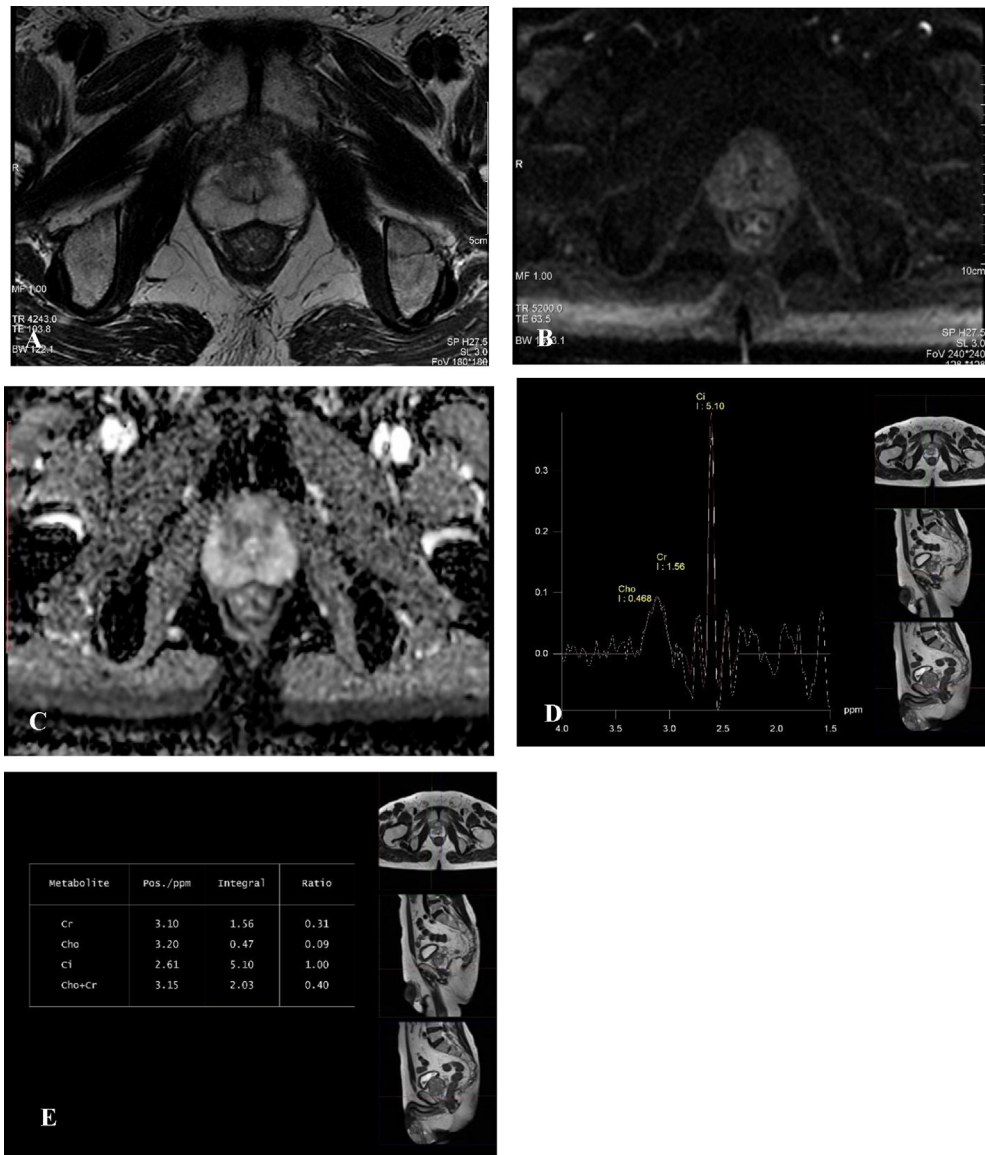

Fig. 3. Multiparametric MR images of a normal prostate. The peripheral zone shows the high signal intensity on the T2WI and ADC map. The MRS images shows prominent citrate peak at a frequency of 2.6 ppm and choline peak at 3.2 ppm. (A) Axial T2WI, (B) Axial DWI, (C) Axial ADC, (D) MRS, (E) MRS biochemical parameter. Cr. = Creatinine, Cho. = Choline, Ci. = Citrate.

peripheral zone of the prostate. Prostate cancer (Fig. 4A) and other benign condition like scar tissue, atrophy, post radiation changes and hormonal treatment effect also often present as a region of low signal intensity on T2WI MR Images [20,21].

The lesion which shows low T2 signal intensity with ill-defined border from the normal part of the peripheral zone of the prostate and the swollen surface but without capsular breach of the organ is interpreted as benign inflammatory
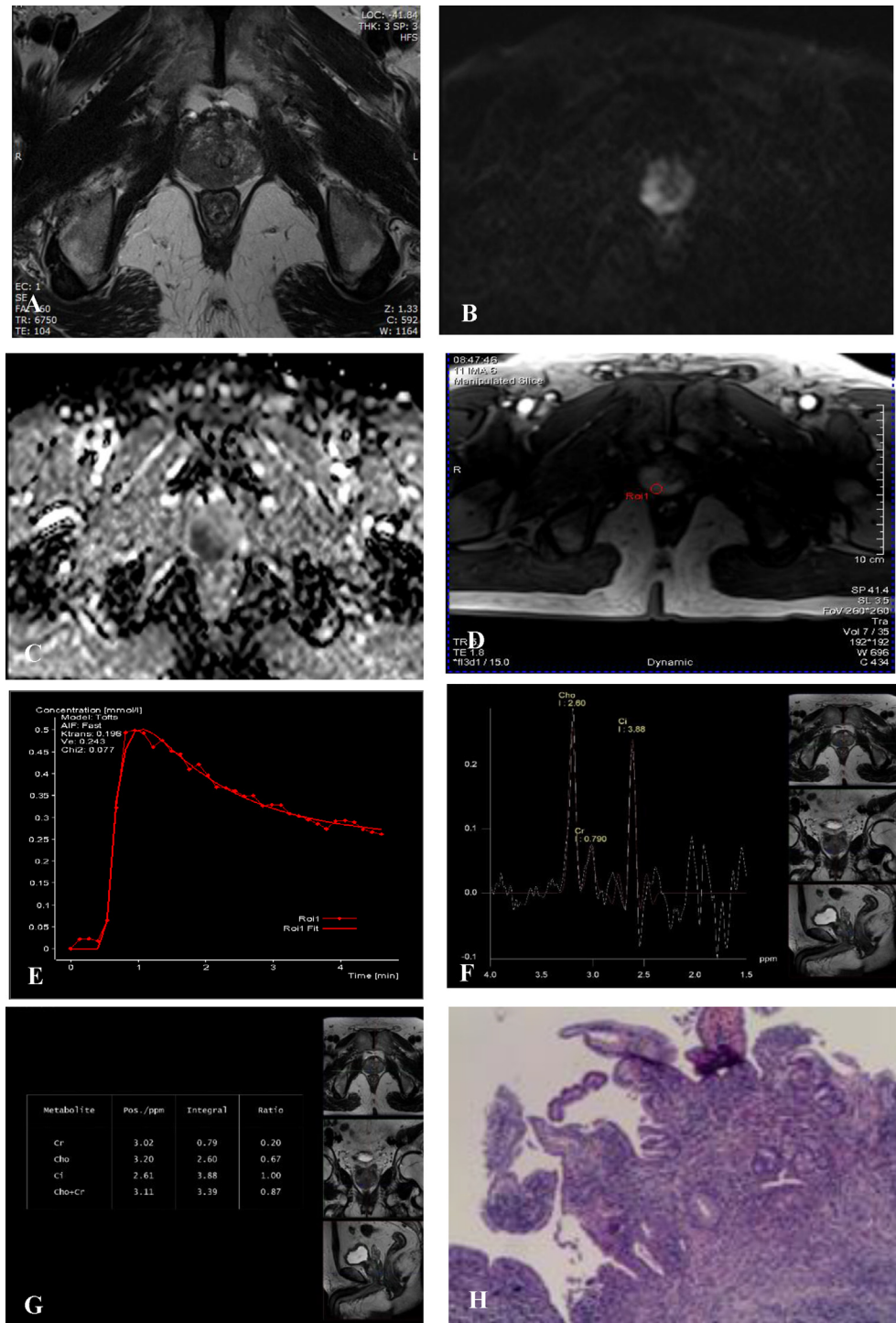

Fig. 4. Multiparametric MR images at 3.0 T without endorectal coils of a 62 years man showing a typical case of prostate cancer located in the peripheral zone. (A) Axial T2WI MR Image shows low signal intensity area in peripheral zone predominantly in the right and extending across the midline to left medial peripheral zone. (B) Axial DWI and (C) Axial ADC map shows corresponding area of high signal intensity and low signal intensity, respectively consistent with restricted diffusion, indicative of tumor. (D) Axial gadolinium based DCE image shows area of early enhancement within corresponding area of restricted diffusion and (E) Curve of the DCE image shows rapid early enhancement with subsequent washout (type IV curve), consistent with tumorous lesion. (F) MRS Image shows elevated choline and creatine peaks with reduced citrate and (G) Value of MRS shows the elevated Cho + Cr/Ci, further supporting the diagnosis of prostate cancer. (H) Histopathology slide confirms the diagnosis.

condition [22]. Likewise, diffuse areas without causing mass effect or wedge shaped areas with low signal intensity are most likely to be chronic prostatitis (Fig. 5A) or other benign conditions [23].

On T2WI MR Images, the central gland which appears as low signal intensity is often intermixed with well circumscribed heterogeneous high and low signal intensity BPH nodules (Fig. 1). A thin boundary of hypo-intense pseudo-
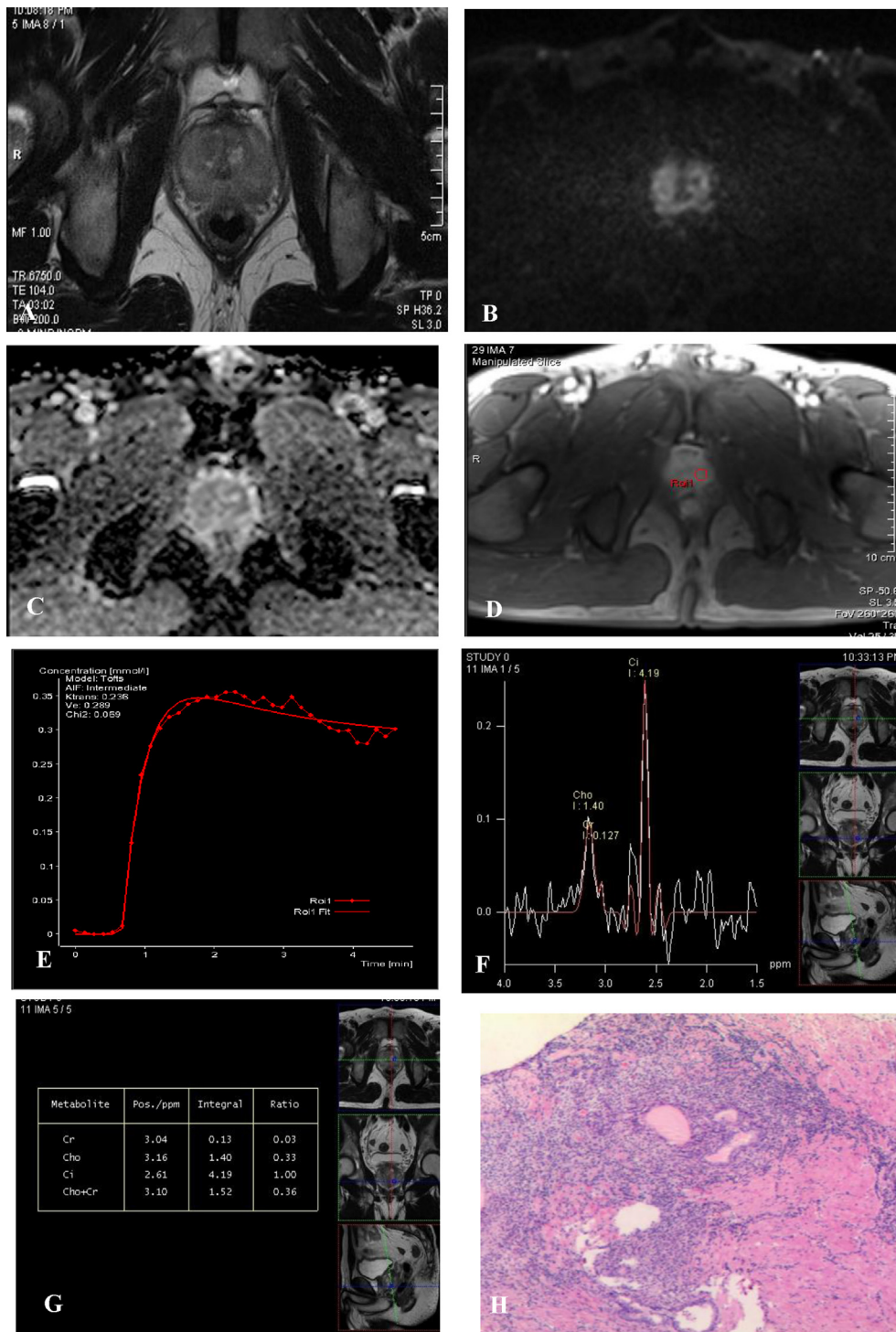

Fig. 5. Multiparametric MR images showing typical chronic prostatitis features in the peripheral zone of the prostate in a 56 year old man, confirmed by histopathology. (A) Axial T2WI MR Image shows diffuse low signal intensity of the bilateral peripheral zone of prostate. (B) Axial DWI and (C) Axial ADC map demonstrate restricted diffusion with low ADC map (however, compared to previous one ADC is not too low), suggestive more of prostatitis. (D) Axial DCE image and (E) Curve of the DCE image demonstrate early enhancement with retaining the contrast (type II curve), consistent with non-tumorous lesion leading to diagnosis of chronic prostatitis. (F) MRS curve and (G) Value of MRS show low peak value of choline and creatine and high peak value of citrate with low Cho + Cr/Ci ratio, ruling out prostate cancer and leading to diagnosis of prostatitis. (H) Histopathology slide confirms the inflammatory process confirming chronic prostatitis.

capsule surrounds the central gland and makes the peripheral zone to be well distinguished from it [15]. Due to the heterogeneous appearance, the identification of prostate cancer in the central gland is very challenging and relatively difficult.

3.2. T1WI MR imaging

The normal appearance of the prostate on T1WI MR Images is homogenously iso-intense and the detailed architectural assessment is almost impossible. So this sequence provides little to no utility in the detection of the suspicious lesions. However, T1WI MR Images can be used to evaluate the hemorrhagic foci as this appear as hyper-intense lesions and also helpful to evaluate nodal involvement.

3.3. DWI MR imaging

On DWI MR Images, the normal tissue appears as low signal intensity or unrestricted due to random Brownian movement of water molecules. Tissues with high cellular density but intact cell membranes like cancerous tissue, abscess, fibrosis or cytotoxic edema appear as high signal intensity or restricted due to inability of water molecules to diffuse freely. Depending on the magnetic field strength and the b-value, the sensitivity of the DWI MR Images vary. Apparent diffusion coefficient (ADCs) map, which is inversely proportional to the degree of diffusion, can be calculated on the basis of DWI MR Images. Low ADC values, which are hypo-intense on the ADC map, and high ADC values, which are hyper-intense on the ADC map, represent tissues with and without restriction of water diffusion, respectively [24]. The peripheral zone of prostate is highly rich in fluid filled tubular tissue owing to homogenously unrestricted diffusion, appearing as low signal intensity on the DWI MR Images and high ADC values (Fig. 3B and C). The central gland is richer in compact smooth muscle rather than glandular tissue in comparison to the peripheral zone, owing to higher percentage of intracellular than extracellular fluid [16]. Further, the ADC values of both the central gland and the peripheral zone increase with age, due to the atrophic changes with ages.

Chronic prostatitis is a condition in which there is inflammation of the gland with extracellular fluid surrounding the prostatic cells and stromal infiltration of chronic inflammatory cells particularly lymphocytes, plasma cells, macrophages [25]. This results in the destruction of the prostate gland leading to weakening of the water diffusion capability. Due to this, chronic prostatitis presents with lower ADC values (Fig. 5B and C) and granulomatous prostatitis can present with even lower ADC values.

Due to the high cellular density and high nucleus to cytoplasm ratio than the normal prostate tissue, and infiltration of the glandular parenchyma with cancerous cells, the prostate cancer shows lower ADC values (Fig. 4B and C) relative to the normal tissue [26]. DWI shows differences between prostatitis and prostate cancer in both the peripheral zone and central gland, however, usability in clinical practice is limited as a result of significant overlap in ADCs [12].

BPH, on the other hand, is represented as intermixed areas of low and high ADC values. This is due to the variable involvement of the glandular, muscular and stromal elements with hyperplasia of central glands [27].

3.4. DCE MR imaging

Dynamic contrast enhanced MR examination is based on the pharmacokinetic properties of tissues in dynamic uptake and washout of Gadolinium based contrast agent, helping in the differentiation of tissues based on their functional assessment. During the examination, fast T1WI MR Images are repeatedly acquired in different phases viz. before, during and after the injection of the bolus dose (2−4 mL/s) of a Gadolinium based contrast agent. The preferred temporal resolution for images acquisition is less than 15s per acquisition with reason of interest being the prostate and the seminal vesicles during this examination [18].

The rapid intake of contrast showing enhancement and subsequently early and pronounced washout demonstrates increased tumor vascularity in relation to the normal surrounding tissues [28,29] (Fig. 4D and E). In chronic prostatitis, there is proliferation of blood vessels along with fibrous connective tissue resulting in increased blood supply. However, the normal architecture of microcirculation is relatively maintained [30]. Chronic prostatitis usually shows no to mild early enhancement as well as late enhancement retaining it till delay phase [31,32] (Fig 5D and E). On the other hand, the granulomatous prostatitis demonstrates moderate enhancement, which is usually lower than prostate cancer [33]. However, it has been reported that DCE MR Images has better diagnostic importance in comparison to T2WI images alone [34,35].

3.5. MR spectroscopic imaging

MR spectroscopy is based on the quantitative differences in the proton precessing frequency of different composing elements of the tissue. The chemical shift, which is compound-specific biochemical analysis, occurs due to the compound specific insulation from Bo. The MR spectroscopy allows detection of citrate and choline in prostate tissue. Citrate is present in high level (>60 mM) in normal prostate tissue due to which the citrate peak is present at a frequency of 2.6 ppm [36]. The decreased levels are seen in case of chronic prostatitis as well as in prostate cancer. Choline peak is present at a frequency of 3.2 ppm in normal prostate tissue, however, the peak is often elevated in case of prostatitis as well as in prostate cancer [25,37,38]. Creatine, a metabolic byproduct, peaks at frequency of 3.0 ppm and the level is low in both normal and prostate cancer without significant difference [39,40]. Since it is difficult to resolve choline peak from creatine, both are evaluated together in prostate MR spectroscopy. Polyamines, regulating molecules for cell proliferation and differentiation, peak at frequency of 3.1 ppm normally and is found to be reduced or absent in prostate cancer [41]. Cho + Cr/Ci ratio is calculated both

quantitatively and qualitatively, on the basis of area under curve and peak heights respectively [13,18,42]. The prostatitis (Fig. 5F and G) is highly suggestive if choline plus creatine to citrate (Cho + Cr/Ci) ratio is not elevated and the diagnosis of prostate cancer (Fig. 4F and G) can be ruled out [39,43,44].

4. MR image guided biopsy

TRUS guided biopsies have low detection rate and its performance can be affected by under sampling and under-scoring of the cancerous process [45,46]. MR images can be helpful in obtaining targeted biopsies to rule out lesions suspicious for cancer.

5. Summary

Multiparametric MR imaging uses the conventional as well as the functional MR Imaging sequences acquired in high field strength of 1.5 T or 3.0 T MR. Multiparametric MR imaging clearly depicts the normal anatomy of the prostate and demonstrates the morphological characteristics of chronic prostatitis and other prostatic disorders. After combining the MR imaging features of all the sequences, chronic prostatitis can be more or less differentiated from other prostate pathology. In case of suspicion for prostate cancer, multiparametric MRI can be helpful in obtainingtargetedbiopsies of the suspicious lesion for histo-pathological examination.

In conclusion, multiparametric MRI can be the best imaging modality for the assessment and diagnosis of chronic prostatitis and its differentiation from prostate cancer.

Acknowledgment

References

[1] Krieger JN, Nyberg Jr L, Nickel JC. NIH consensus definition and classification of prostatitis. Jama 1999;282(3):236—7.

[2] Murphy AB, Macejko A, Taylor A, Nadler RB. Chronic prostatitis: management strategies. Drugs 2009;69(1):71—84.

[3] Nickel JC. Clinical evaluation of the man with chronic prostatitis/chronic pelvic pain syndrome. Urology 2002;60(6 Suppl.):20—2. discussion 2—3.

[4] Nadler RB, Collins MM, Propert KJ, Mikolajczyk SD, Knauss JS, Landis JR, et al. Prostate-specific antigen test in diagnostic evaluation of chronic prostatitis/chronic pelvic pain syndrome. Urology 2006;67(2):337—42.

[5] Mahal BA, Cohen JM, Allsop SA, Moore JB, Bhai SF, Inverso G, et al. The role of phenotyping in chronic prostatitis/chronic pelvic pain syndrome. Curr Urol Rep 2011;12(4):297—303.

[6] Sperandeo G, Sperandeo M, Morcaldi M, Caturelli E, Dimitri L, Camagna A. Transrectal ultrasonography for the early diagnosis of adenocarcinoma of the prostate: a new maneuver designed to improve the differentiation of malignant and benign lesions. J Urol 2003;169(2):607—10.

[7] Ikonen S, Kivisaari L, Tervahartiala P, Vehmas T, Taari K, Rannikko S. Prostatic MR imaging. Accuracy in differentiating cancer from other prostatic disorders. Acta Radiol 2001;42(4):348—54.

[8] Rifkin MD, Zerhouni EA, Gatsonis CA, Quint LE, Paushter DM, Epstein JI, et al. Comparison of magnetic resonance imaging and ultrasonography in staging early prostate cancer. Results of a multi-institutional cooperative trial. N Engl J Med 1990;323(10):621—6.

[9] Ahmed HU, Emberton M. The role of magnetic resonance imaging in targeting prostate cancer in patients with previous negative biopsies and elevated prostate-specific antigen levels. BJU Int 2009;104(2):269—70. author reply 70.

[10] Lawrentschuk N, Fleshner N. The role of magnetic resonance imaging in targeting prostate cancer in patients with previous negative biopsies and elevated prostate-specific antigen levels. BJU Int 2009;103(6):730—3.

[11] Habchi H, Bratan F, Paye A, Pagnoux G, Sanzalone T, Mege-Lechevallier F, et al. Value of prostate multiparametric magnetic resonance imaging for predicting biopsy results in first or repeat biopsy. Clin Radiol 2014;69(3):e120—8.

[12] Nagel KN, Schouten MG, Hambrock T, Litjens GJ, Hoeks CM, ten Haken B, et al. Differentiation of prostatitis and prostate cancer by using diffusion-weighted MR imaging and MR-guided biopsy at 3 T. Radiology 2013;267(1):164—72.

[13] Chen ME, Johnston DA, Tang K, Babaian RJ, Troncoso P. Detailed mapping of prostate carcinoma foci: biopsy strategy implications. Cancer 2000;89(8):1800—9.

[14] McNeal JE, Redwine EA, Freiha FS, Stamey TA. Zonal distribution of prostatic adenocarcinoma. Correlation with histologic pattern and direction of spread. Am J Surg Pathol 1988;12(12):897—906.

[15] Coakley FV, Hricak H. Radiologic anatomy of the prostate gland: a clinical approach. Radiol Clin N Am 2000;38(1):15—30.

[16] Hricak H, Dooms GC, McNeal JE, Mark AS, Marotti M, Avallone A, et al. MR imaging of the prostate gland: normal anatomy. AJR Am J Roentgenol 1987;148(1):51—8.

[17] McNeal JE. Normal anatomy of the prostate and changes in benign prostatic hypertrophy and carcinoma. Semin Ultrasound, CT, MR 1988;9(5):329—34.

[18] Barentsz JO, Richenberg J, Clements R, Choyke P, Verma S, Villeirs G, et al. ESUR prostate MR guidelines 2012. Eur Radiol 2012;22(4):746—57.

[19] de Bazelaire CM, Duhamel GD, Rofsky NM, Alsop DC. MR imaging relaxation times of abdominal and pelvic tissues measured in vivo at 3.0 T: preliminary results. Radiology 2004;230(3):652—9.

[20] Quint LE, Van Erp JS, Bland PH, Del Buono EA, Mandell SH, Grossman HB, et al. Prostate cancer: correlation of MR images with tissue optical density at pathologic examination. Radiology 1991;179(3):837—42.

[21] Wang L, Mazaheri Y, Zhang J, Ishill NM, Kuroiwa K, Hricak H. Assessment of biologic aggressiveness of prostate cancer: correlation of MR signal intensity with Gleason grade after radical prostatectomy. Radiology 2008;246(1):168—76.

[22] Szolar DH, Ranner G, Preidler KW, Lax S. Non-granulomatous prostatitis: MRI image with endorectal surface coil ("Endo-MRI"). Aktuelle Radiol 1995;5(1):67—9.

[23] Cruz M, Tsuda K, Narumi Y, Kuroiwa Y, Nose T, Kojima Y, et al. Characterization of low-intensity lesions in the peripheral zone of prostate on pre-biopsy endorectal coil MR imaging. Eur Radiol 2002;12(2):357—65.

[24] Qayyum A. Diffusion-weighted imaging in the abdomen and pelvis: concepts and applications. Radiographics 2009;29(6):1797—810.

[25] Shukla-Dave A, Hricak H, Eberhardt SC, Olgac S, Muruganandham M, Scardino PT, et al. Chronic prostatitis: MR imaging and 1H MR spectroscopic imaging findings—initial observations. Radiology 2004;231(3):717—24.

[26] Anderson AW, Xie J, Pizzonia J, Bronen RA, Spencer DD, Gore JC. Effects of cell volume fraction changes on apparent diffusion in human cells. Magn Reson Imaging 2000;18(6):689—95.

[27] Ren J, Huan Y, Wang H, Zhao H, Ge Y, Chang Y, et al. Diffusion-weighted imaging in normal prostate and differential diagnosis of prostate diseases. Abdom Imaging 2008;33(6):724—8.

[28] Franiel T, Ludemann L, Rudolph B, Rehbein H, Staack A, Taupitz M, et al. Evaluation of normal prostate tissue, chronic prostatitis, and prostate cancer by quantitative perfusion analysis using a dynamic contrast-enhanced inversion-prepared dual-contrast gradient echo sequence. Invest Radiol 2008;43(7):481—7.

[29] Barentsz JO, Engelbrecht M, Jager GJ, Witjes JA, de LaRosette J, van Der Sanden BP, et al. Fast dynamic gadolinium-enhanced MR imaging of urinary bladder and prostate cancer. J Magn Reson Imaging 1999;10(3):295–304.

[30] Lovett K, Rifkin MD, McCue PA, Choi H. MR imaging characteristics of noncancerous lesions of the prostate. J Magn Reson Imaging 1992; 2(1):35–9.

[31] Kim CK, Park BK, Kim B. Localization of prostate cancer using 3T MRI: comparison of T2-weighted and dynamic contrast-enhanced imaging. J Comput Assist Tomogr 2006;30(1):7–11.

[32] Engelbrecht MR, Huisman HJ, Laheij RJ, Jager GJ, van Leenders GJ, Hulsbergen-Van De Kaa CA, et al. Discrimination of prostate cancer from normal peripheral zone and central gland tissue by using dynamic contrast-enhanced MR imaging. Radiology 2003;229(1):248–54.

[33] Bott SR, Ahmed HU, Hindley RG, Abdul-Rahman A, Freeman A, Emberton M. The index lesion and focal therapy: an analysis of the pathological characteristics of prostate cancer. BJU Int 2010;106(11): 1607–11.

[34] Futterer JJ, Heijmink SW, Scheenen TW, Veltman J, Huisman HJ, Vos P, et al. Prostate cancer localization with dynamic contrast-enhanced MR imaging and proton MR spectroscopic imaging. Radiology 2006;241(2):449–58.

[35] Ocak I, Bernardo M, Metzger G, Barrett T, Pinto P, Albert PS, et al. Dynamic contrast-enhanced MRI of prostate cancer at 3 T: a study of pharmacokinetic parameters. AJR Am J Roentgenol 2007;189(4):849.

[36] Costello LC, Franklin RB. The intermediary metabolism of the prostate: a key to understanding the pathogenesis and progression of prostate malignancy. Oncology 2000;59(4):269–82.

[37] Podo F. Tumour phospholipid metabolism. NMR Biomed 1999;12(7):413–39.

[38] Glunde K, Ackerstaff E, Mori N, Jacobs MA, Bhujwalla ZM. Choline phospholipid metabolism in cancer: consequences for molecular pharmaceutical interventions. Mol Pharm 2006;3(5):496–506.

[39] Kurhanewicz J, Vigneron DB, Hricak H, Narayan P, Carroll P, Nelson SJ. Three-dimensional H-1 MR spectroscopic imaging of the in situ human prostate with high (0.24–0.7-cm^3) spatial resolution. Radiology 1996;198(3):795–805.

[40] Fuchsjager M, Shukla-Dave A, Akin O, Barentsz J, Hricak H. Prostate cancer imaging. Acta Radiol 2008;49(1):107–20.

[41] Shukla-Dave A, Hricak H, Moskowitz C, Ishill N, Akin O, Kuroiwa K, et al. Detection of prostate cancer with MR spectroscopic imaging: an expanded paradigm incorporating polyamines. Radiology 2007;245(2): 499–506.

[42] Villeirs GM, Oosterlinck W, Vanherreweghe E, De Meerleer GO. A qualitative approach to combined magnetic resonance imaging and spectroscopy in the diagnosis of prostate cancer. Eur J Radiol 2010;73(2):352–6.

[43] Jung JA, Coakley FV, Vigneron DB, Swanson MG, Qayyum A, Weinberg V, et al. Prostate depiction at endorectal MR spectroscopic imaging: investigation of a standardized evaluation system. Radiology 2004;233(3):701–8.

[44] Scheenen TW, Futterer J, Weiland E, van Hecke P, Lemort M, Zechmann C, et al. Discriminating cancer from noncancer tissue in the prostate by 3-dimensional proton magnetic resonance spectroscopic imaging: a prospective multicenter validation study. Invest Radiol 2011;46(1):25–33.

[45] Chun FK, Epstein JI, Ficarra V, Freedland SJ, Montironi R, Montorsi F, et al. Optimizing performance and interpretation of prostate biopsy: a critical analysis of the literature. Eur Urol 2010;58(6):851–64.

[46] Hambrock T, Hoeks C, Hulsbergen-van de Kaa C, Scheenen T, Futterer J, Bouwense S, et al. Prospective assessment of prostate cancer aggressiveness using 3-T diffusion-weighted magnetic resonance imaging-guided biopsies versus a systematic 10-core transrectal ultrasound prostate biopsy cohort. Eur Urol 2012;61(1):177–84.